Chemico-Biological Interactions 182 (2009) 136–147

Contents lists available at ScienceDirect

Chemico-Biological Interactions

journal homepage: www.elsevier.com/locate/chembioint

Superoxide anion mediated mitochondrial dysfunction leads to hepatocyte apoptosis preferentially in the periportal region during copper toxicity in rats

Dijendra Nath Roy, Samir Mandal, Gargi Sen, Tuli Biswas*

Indian Institute of Chemical Biology, CSIR, Kolkata 700032, India

ARTICLE INFO

Article history:
Received 2 July 2009
Received in revised form 18 August 2009
Accepted 19 August 2009
Available online 26 August 2009

Keywords:
Copper toxicity
Superoxide anion
Hepatocyte apoptosis
Periportal region
Mitochondrial dysfunction

ABSTRACT

Chronic exposure to copper induces hepatocellular apoptosis with greater injury in the periportal region compared to the perivenous region. Here we have identified the factors responsible for the development of regional damage in the liver under *in vivo* conditions. Enhanced production of reactive oxygen species (ROS) with predominance of superoxide radical ($O_2^{\bullet -}$) indicates the contribution of redox imbalance in the process. This may be linked with copper catalyzed oxidation of GSH to GSSG resulting in the generation of $O_2^{\bullet -}$. Downregulation of Cu-Zn SOD in consequence of the degradation of this enzyme, causes decreased dismutation of $O_2^{\bullet -}$, that further contributes to the enhanced level of $O_2^{\bullet -}$ in the periportal region. Decreased functioning of Mn SOD activity, reduction in mitochondrial thiol/disulphide ratio and generation of $O_2^{\bullet -}$ were much higher in the mitochondria from periportal region, which point to the involvement of this organelle in the regional hepatotoxicity observed during copper exposure. This was supported by copper-mediated enhanced mitochondrial dysfunction as evident from ATP depletion, collapse of mitochondrial membrane potential (MMP) and induction of mitochondrial permeability transition (MPT). Results suggest the active participation of $O_2^{\bullet -}$ in inducing mitochondrial dysfunction preferentially in the periportal region that eventually leads to the development of hepatotoxicity due to copper exposure under *in vivo* condition.

1. Introduction

Diseases like Wilson Disease, Indian Childhood Cirrhosis, Idiopathic Copper Toxicosis and Chronic Cholestasis are all associated with hepatic copper accumulation which eventually leads to cirrhosis of the liver [1,2,3]. Copper is absorbed from the gastrointestinal tract and transported to the hepatocytes via portal transporters. Intracellular copper then binds to metalochaperones and becomes destined for storage within hepatocytes, secretion in plasma or excretion in bile [4]. Although liver is considered to be the main site for copper homeostasis in the body, excess of this transition metal induces apoptotic changes in the hepatocytes followed by cirrhosis which eventually culminates in liver failure [5].

Hepatocytes display distinct heterogeneity towards structure and function within different zones of the liver [6,7]. Even though wide variance has been observed in metabolic and transport processes specifically between the periportal and perivenous regions, it is not yet clear whether this zonal dissimilarity has any reflection on the cellular death process associated with hepatotoxicity. Keeping this in mind, the first aim of our study was to find out the response of hepatocytes from periportal and perivenous regions in copper toxicity under *in vivo* conditions.

Recent reports implicate mitochondria as the major target for liver toxicity resulting from copper overload, either through high dietary intake or due to a genetic defect in transport mechanism [8]. However, the sequence of events in the development of pathologies related to mitochondrial dysfunction with an emphasis on its applicability under *in vivo* conditions remained largely unknown.

Literature available so far suggests that dissipation of mitochondrial transmembrane potential ($\Delta\psi_m$), followed by induction of mitochondrial permeability transition (MPT) eventually lead to the release of proapoptotic factors and activate cellular apoptosis [9]. Whilst the redox property of copper is essential for the activity of cuproenzymes, excess of this element in the cells can also be a source of reactive oxygen species (ROS), that can damage lipids, proteins and nucleic acids [10]. Since enhanced generation of ROS

Abbreviations: $CuSO_4$, copper sulphate; RPMI 1640, Roswell Park Memorial Institute 1640; FBS, fetal bovine serum; ALT, alanine transaminase; PP, periportal; PV, perivenous; HEPES, N-(2-hydroxyethyl)-piperazine-N′-2-ethanesulphonic acid; EDTA, ethylene diamine tetraacetic acid; EGTA, ethylene glycol tetraacetic acid; DTT, dithiothreitol; TBARS, thiobarbituric acid reactive substance; DHE, dihydroethidium; DCFDA, 2′,7′-dichlorofluorescein diacetate; $O_2^{\bullet -}$, superoxide; H_2O_2, hydrogen peroxide; DTNB, 5,5'-dithiobis-(2-nitrobenzoic acid); NEM, N-ethyl maleimide; GAPDH, glyceraldehyde 3-phosphate dehydrogenase; Rh-123, Rhodamine 123.

* Corresponding author at: Cell Biology and Physiology Division, Indian Institute of Chemical Biology, CSIR, 4, Raja S.C. Mullick Road, Kolkata 700032, India. Tel.: +91 33 2473 3491; fax: +91 33 2473 0284.
E-mail address: tulibiswas@iicb.res.in (T. Biswas).

0009-2797/$ – see front matter © 2009 Elsevier Ireland Ltd. All rights reserved.
doi:10.1016/j.cbi.2009.08.014

is known to play an important role in MPT induction, our second aim was to explore whether copper toxicity can induce ROS mediated MPT opening followed by mitochondrial dysfunction, and to identify the ROS involved in the process.

In the presence of glutathione (GSH), Cu^{2+} is reduced to Cu^{+} which then catalyzes the generation of ROS via the Fenton reaction. Considering the importance of GSH in the mobilization of copper in hepatocytes [11], our third objective was to determine whether GSH is involved in the generation of ROS and induction of mitochondrial dysfunction that may ultimately converge to hepatocyte apoptosis during copper toxicity.

2. Materials and methods

2.1. Chemicals

Unless otherwise noted, all chemicals were obtained from Sigma (St. Louis, MO). RPMI Medium 1640 (GIBCO™) and FBS (GIBCO™) were obtained from Invitrogen Corporation (Grand Island, NY). Serum Alanine Transaminase (ALT) measurement kit was obtained from TECO Diagnostics (Anaheim, CA). ATP Bioluminescence Assay Kit was purchased from Biovision Inc. (Mountain View, CA). TUNEL assay kit (APO-DIRECT™ kit) was purchased from Calbiochem (San Diego, CA). The primary antibody [SOD-1 (FL-154); Santa Cruz Biotechnology Inc.] for SOD1 was obtained from Santa Cruz, CA and the primary antibody (mAbcam-9485; Abcam Inc.) for GAPDH was obtained from Cambridge, MA. Copper sulphate pure ($CuSO_4$, $5H_2O$) was purchased from Sisco Research Laboratory Pvt. Ltd. (Mumbai, India).

2.2. Animals and treatment

Male Sprauge–Dawley rats (45–55 g) were given standard laboratory diet and water ad libitum. All animals were bred and housed in the animal house of Indian Institute of Chemical Biology, Kolkata. They were kept in an environment of constant temperature and humidity with 12 h day–night cycle. All animal studies were performed following the mandates approved by Animal Ethics Committee (Committee for the purpose of control and supervisions of experiments of animals, Govt. of India).

Animals were grouped according to drug treatment with 6 animals in each group. Copper sulphate ($CuSO_4$) was dissolved in 0.9% NaCl and administered everyday by gavage in doses ranging from 10 to 20 mg/kg for different time periods up to 90 days for assessing their mean survival time against copper exposure. For all other experiments animals were given $CuSO_4$ at a dose of 15 mg/kg for 45 days. Selection of this dose for the development of copper toxicity was based on an integrated overview of the physiologic and pathologic responses associated with range of copper intake. This is also in well accordance with the daily intake of greater than 5 mg/kg as suggested by Aggett [12] for development of copper toxicity. In the D-penicillamine treated groups the treatment with it was started at a dose of 10 mg/kg, ip. b.d. thrice a week after 15 days of $CuSO_4$ exposure and continued till the last day of $CuSO_4$ exposure in the respective groups. The dose used by us is in well accordance with the recommended dose of D-penicillamine for chronic treatment [13,14]. Consistent with these reports, this low dose of D-penicillamine appeared to be most suitable which reduced the adverse effect of the drug without compromising the efficacy. To ascertain this we have done blood count, renal function test and behavioral study periodically in the animals undergoing treatment. This dose is also compatible with the report of Brewer [15] suggesting a dose 250 mg × 4 times a day for adult person which is equivalent to a dose of approximately 20 mg/kg. Reports on neurologic symptoms are essentially applicable to the patients already suffering from neurologic disorders and whose condition deteriorated after the treatment. Apart from this, reports on the side effect at this low dose are very few. Rats in the control group received equivalent level of 0.9% NaCl on the same days. Animals were sacrificed 24 h after the last dose of exposure.

2.3. Primary hepatocyte culture

Hepatocytes were isolated from rat livers following standard two step collagenase perfusion technique [16,17]. Cells were plated in a 24-well collagenase coated culture dish at a density of 8×10^4 cells in 0.4 ml/well and were cultured in RPMI 1640 medium (GIBCO™) supplemented with 10% (v/v) heat inactivated fetal bovine serum (FBS), 100 U/ml penicillin and 100 mg/ml streptomycin at 37 °C in a humidified atmosphere of 5% CO_2 in air. The medium was then changed every 24 h with the exclusion of FBS and inclusion of insulin (0.1 μM) [18]. Cell viability was between 85% and 95% as determined by trypan blue exclusion.

2.4. Measurement of Serum Alanine Transaminase (ALT)

The activity of ALT (EC2.6.1.2) was determined colorimetrically according to standard procedures using commercially available diagnostic laboratory kit.

2.5. Histopathological study

Tissues from liver were fixed in Bouin's solution followed by dehydration and were then embedded in paraffin. 5 μm sections were cut and stained with hematoxylin and eosin for histological examinations. For histochemical studies, sections were stained with Rhodanine to demonstrate copper deposition. Slides were examined under light microscope (Model BX51 TRF, Olympus, Japan).

2.6. Isolation of periportal and perivenous hepatocytes

PP and PV hepatocytes were isolated following digitonin-collagenase perfusion method [17]. Briefly, inferior vena cava, superior vena cava and portal vein were first cannulated. For the isolation of PP cells, 1 mM digitonin solution (prepared by boiling in Hanks' solution) was infused at 37 °C into the inferior vena cava for 10 s followed by Ca^{2+} free Hanks buffer for 3 min. Collagenase (95 U/ml) was then infused for 7 min through portal cannula. Cells were then dispersed in Eagle's minimum essential medium, filtered through gauge mesh and washed four times by centrifugation at $50 \times g$ for 1 min. For the isolation of PV cells, same procedure was followed, except the direction of perfusion comprising digitonin and collagenase infusion were reversed. Cell viability was determined by trypan blue exclusion.

2.7. Isolation of mitochondria and cytosolic fraction

All the procedures were carried out at 4 °C. Mitochondria was isolated by a small modification of Tay et al. [19]. Cells were suspended in a fresh serum based medium (20 mM HEPES, 10 mM KCl, 1.5 mM $MgCl_2$, 1 mM EDTA, 1 mM EGTA, 1 mM DTT and 250 mM sucrose, pH7.4) and gently homogenized. The homogenate was centrifuged at $800 \times g$ for 10 min. The supernatant was centrifuged at $10{,}000 \times g$ for 10 min and the resulting pellet was washed by resuspension in wash buffer (210 mM mannitol, 70 mM sucrose, 5 mM HEPES, pH 7.4) and centrifuged at $10{,}000 \times g$ for 10 min. The mitochondrial pellet was suspended in wash buffer and kept at −80 °C for further use.

Cytosolic fraction was isolated according to Domenicotti et al. [20] with a minor modification [21]. Cells were suspended in bufferA (50 mM Tris–HCl, pH 7.5,100 mM NaCl, 10 mM EDTA and

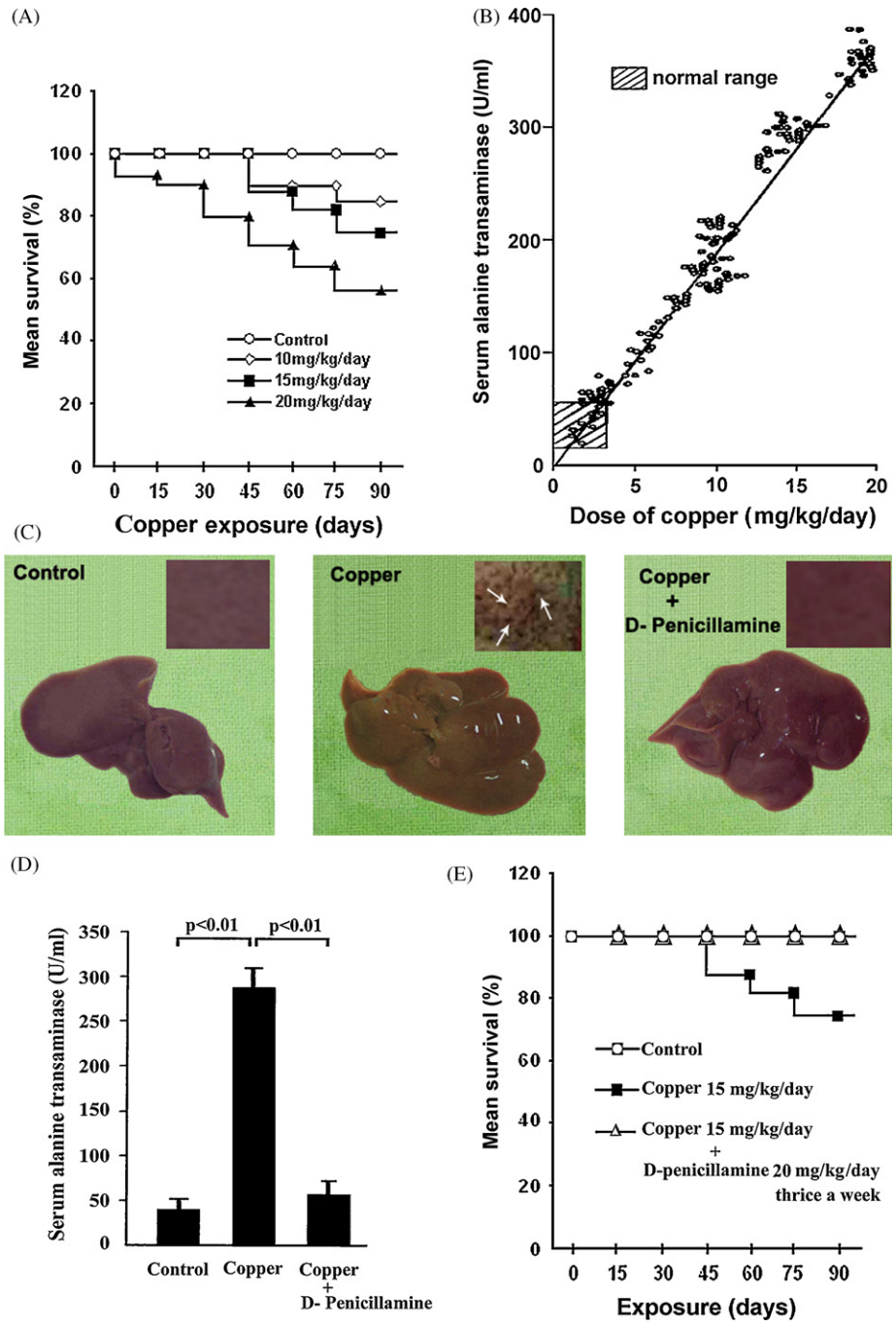

Fig. 1. Chronic exposure to copper increases rat mortality in association with altered liver morphology and enhanced hepatotoxicity. (A) Survival curve shows % survival of rats exposed to increasing doses of copper for a period of 90 days. (B) Correlation between serum ALT activity, an index of copper hepatotoxicity and different doses of copper exposure (1–20 mg/kg/day) for a period of 45 days. (C) Changes in liver morphology of control rats in response to copper exposure (15 mg/kg/day for 45 days) and its successful rectification with D-penicillamine treatment. Inset figure shows nailed appearance (indicated with arrows) in copper-exposed rat liver. (D) Serum ALT activity in the copper-exposed rats with and without D-penicillamine treatment. (E) Effect of D-penicillamine treatment on the % survival on rats subjected to copper exposure for 90 days. The values are the mean ± SD of five independent observations with 6 animals per group.

2.5%, v/v Triton-X 100) containing 1/1000 (v/v) protease inhibitor cocktail. It was then shaken for 15 min at room temperature and sonicated four times 15 s each time. After centrifugation at 10,000 × *g* for 10 min, the supernatant containing cytosolic fraction was stored at −80 °C until use.

2.8. Estimation of copper

Aliquots of mitochondrial and cytosolic fraction were freeze dried, transferred to quartz vessel and weighed. Organic material was destroyed by plasma oxidation at low temperature. The residue was dissolved in 12N nitric acid. Copper content was determined by Atomic Absorption Spectroscopy (model: Analyst 200, PerkinElmer) [22].

2.9. Determination of ATP production

ATP production was measured using ATP Bioluminescence Assay Kit (Biovision) according to manufacturer's instruction. Briefly, 1 μg of mitochondrial protein was added to 200 μl of

reaction mixture supplemented with 2.5 mM glutamate and 2.5 mM malate. The reaction was initiated with the addition of ADP to a final concentration of 6.25 mM. The luminescence was followed at 560 nm. ATP production was determined in terms of nmol of ATP/mg of mitochondrial protein/min.

2.10. Measurement of lipid peroxidation

Lipid peroxidation was determined from the amount of thiobarbituric acid reactive substance (TBARS) formed in hepatocytes plasma membrane isolated by following the method of Hubbard et al. [23]. Values were expressed as nmol of TBARS per mg protein using molar extinction coefficient of $1.56 \times 10^5\ M^{-1}\ cm^{-1}$ [24].

2.11. Assessment of nuclear morphology

Nuclear morphology of cell was studied after staining with Hoechst 33342 (bisbenzimide H33342 Fluorochrome) [25]. Hoechst 33342 was added to the hepatocytes at a final concentration of 10 μg/ml and incubated at 37 °C. After 30 min, number of cells with apoptotic nuclei was determined by counting per 100 cells chosen randomly under confocal microscope (Zeiss LSM 510 model, Oberkochen, Germany).

2.12. Terminal deoxynucleotide transferase (Tdt) mediated dUTP-nick end-labeling (TUNEL) assay

DNA fragmentation was determined using TUNEL assay according to the manufacturer protocol (*In situ* cell death detection kit; APO-DIRECT™ kit, Calbiochem, USA). Briefly, fixed cells were incubated at 37 °C for 1 h with Tdt buffer containing FITC-labeled dUTP. Cells were counter stained with PI and analyzed with FACS scan (Becton Dickinson; FACS calibur, BD Bioscience) equipped with 488 nm argon laser. Cells are displayed as DNA area (linear red fluorescence) on the *X*-axis versus FITC-dUTP (log green fluorescence) on the *Y*-axis. A horizontal gate was applied to this display to discriminate between apoptotic (FITC staining) and non-apoptotic cells.

2.13. Measurement of intracellular ROS

The level of intracellular ROS was determined by incubating cells with fluorescent probe dihydroethidium (DHE) or 2′,7′-dichlorofluorescein diacetate (DCFDA) followed by the measurement of the oxidation of DHE to ethidium (ETH) by $O_2^{\bullet -}$ or DCFDA to dichlorofluorescin (DCF) by H_2O_2. Mitochondrial superoxide was assessed by incubating mitochondria with DHE only [26]. Samples were analyzed with an excitation wavelength of 488 nm and emission wavelengths of 585 nm for $O_2^{\bullet -}$ and 525 nm for H_2O_2. Analyses of *in vivo* experiments were made with flow cytometer (Becton Dickinson; FACS calibur, BD Bioscience) and of *in vitro* experiment with spectrofluorimeter (PerkinElmer, LS50).

2.14. Cellular glutathione content

Cellular glutathione content was measured as described previously [27]. Briefly, samples were first deproteinized with 35% metaphosphoric acid. The acid supernatant was neutralized with Na_2HPO_4. Total glutathione level was determined after adding DTNB and measuring the formation of glutathione–DTNB conjugate at 412 nm according to the method of Tietze [28]. Oxidized glutathione (GSSG) level was determined enzymatically following the method of Srivastava and Beutler [29]. Reduced glutathione (GSH) was first alkylated with N-ethyl maleimide (NEM). 30% TCA was then added as precipitating agent, followed by centrifugation at $1000 \times g$ for 15 min. Clear supernatant was extracted with ice cold ether to remove TCA and NEM. Excess ether was removed with nitrogen gas. GSSG was assessed from its reduction to GSH catalyzed by glutathione reductase (GR), following the oxidation of NADPH at 340 nm. GSH concentration was determined by subtracting GSSG from total glutathione value in GSH equivalent.

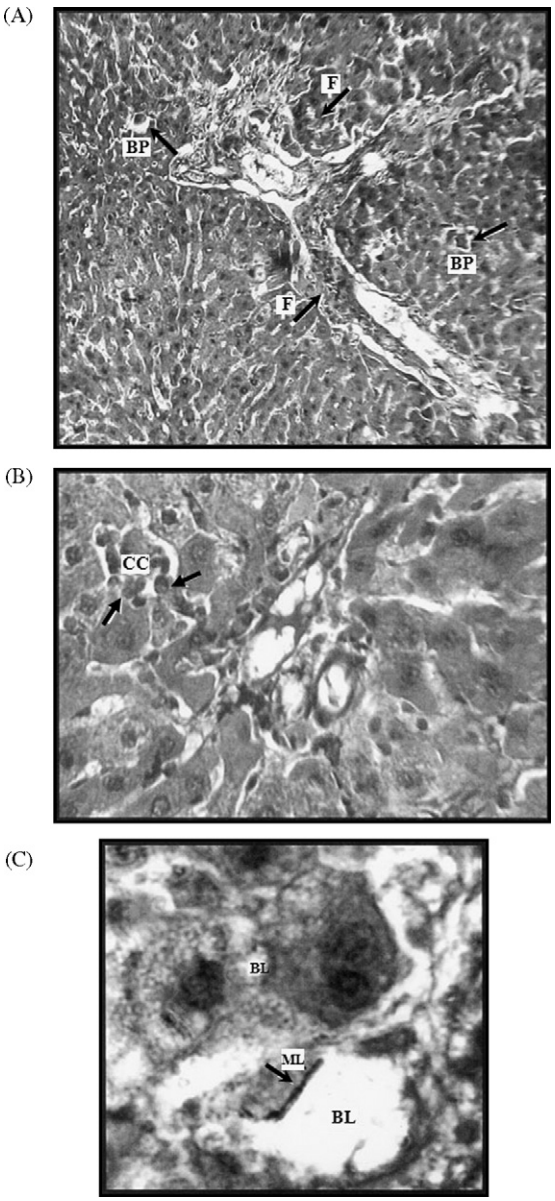

Fig. 2. Effect of copper exposure on liver histology of rats. Photomicrographs of hematoxylin/eosin-stained PP zone of liver from copper-exposed rats show (A). Fibrotic changes (F) indicated with arrows and bile plugs (BP). The magnification of the photomicrograph is 100×. (B) Cholangiolar proliferation (CC) indicated with arrows. The magnification of the photomicrograph is 400×. (C) Ballooning (BL) of hepatocytes and mallory body (ML) formation indicated by arrow. The magnification of the photomicrograph is 1000×. Results are representative of five independent experiments.

2.15. Assay of Cu-Zn SOD and Mn SOD activity

Total SOD activity determined spectrophotometrically following the inhibition of pyrogallol auto oxidation by $O_2^{\bullet -}$ at 420 nm [30]. One unit of SOD represents the amount of enzyme necessary to produce 50% inhibition of $O_2^{\bullet -}$ mediated oxidation of pyrogallol. To

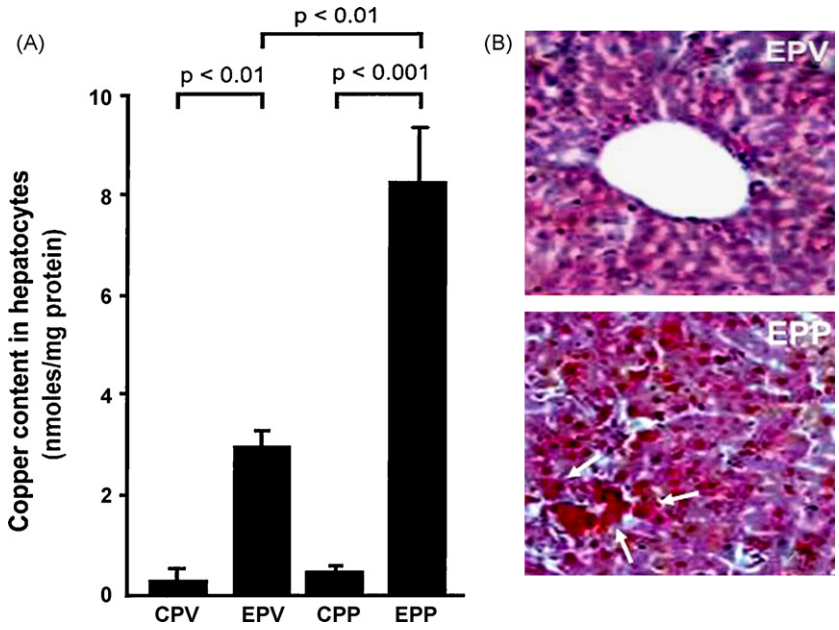

Fig. 3. Zonal distribution of copper in the cytosolic fractions of hepatocytes after chronic exposure. (A) Accumulation of copper in PP and PV hepatocytes from control (CPP and CPV) and copper-exposed rats (EPP and EPV) were estimated in AAS. (B) Photomicrographs of histologic sections stained with 5-(4-dimethylamino benzilidine)-3-(3-methoxypropyle) Rhodanine, confirmed the zonal heterogeneity towards copper deposition. The figure demonstrates marked increase of brick red granules, indicating copper deposition, in EPP region over EPV region. The magnification of the photomicrograph is 800×. Results are representative of five independent experiments.

determine Mn SOD activity, Cu-Zn SOD was totally inhibited (100%) with NaCN. Cu-Zn SOD activity was calculated by subtracting Mn SOD activity from the total SOD activity.

2.16. Western blot of Cu-Zn SOD

Protein bands of Cu-Zn SOD and GAPDH (as internal control) from SDS-PAGE were transferred to nitrocellulose membrane. Membranes were probed using specific primary antibodies against Cu-Zn SOD (Santa Cruz Biotechnology, Santa Cruz, CA) at 1:200 dilution and GAPDH (Abcam) at 1:2500 dilution [31]. Secondary antibody conjugated to alkaline phosphatase was used for detection with NBT/BCIP substrate. Immunoblot band intensities were quantified using ImageJ software.

2.17. Measurement of mitochondrial membrane potential (MMP)

MMP was measured by monitoring fluorescent quenching Rhodamine 123 (Rh-123). Cells were labeled by incubating in a medium containing 1 μM Rh-123 for 15 min at 37 °C. After washing in PBS, samples were analyzed by flow cytometry within 30 min [32]. *In vitro* observations were made spectrofluorimetrically (PerkinElmer LS50) with excitation at 503 nm and emission at 527 nm [33].

2.18. Measurement of mitochondrial permeability transition (MPT)

MPT was measured by recording light scattering results from the swelling of mitochondria. The amount of light scattered is inversely proportional with the mitochondrial volume. MPT induction was monitored from the changes in absorbance at 540 nm over 15 min at room temperature in a UV–vis spectrophotometer (UV-1700 Pharma Spec, Shimadzu) [34].

2.19. Statistical analysis

All data were presented as the mean ± S.D. for the indicated number of experiments and the means were compared by use of ANOVA for statistical analysis of data involving multiple comparisons. Differences between two groups were compared by unpaired Student's *t* test. A value of $p < 0.05$ was considered statistically significant.

3. Results

3.1. Copper toxicity induces morphological and functional alterations in liver

In order to elucidate the mechanism of copper induced liver toxicity under *in vivo* condition, we first determined the endurance of rats towards exposure to increasing doses of copper for different durations. As evident from Fig. 1A, exposure to $CuSO_4$ beyond 45 days affected the mean survival of all the animals. Rats receiving lower doses (10 mg/kg and 15 mg/kg) showed 100% survival up to 45 days, whereas the animals receiving $CuSO_4$ at the dose of 20 mg/kg could not tolerate the treatment showing 20% drop in their survival after similar period of exposure. This made us select 45 days as the period of exposure in our further experiments. We next measured the extent of liver toxicity developed after 45 days of treatment with increasing doses of $CuSO_4$ up to 20 mg/kg. Fig. 1B shows dose dependent increase in ALT activity with significant rise between 15 and 20 mg/kg. Since treatment with 15 mg/kg resulted in conspicuous development of liver toxicity with minimal loss of mean survival, we have used this dose of $CuSO_4$ in all further experiments. The surviving rats had a reduced rate of weight gain during the period of exposure in comparison to the control animals of the same age group. Exposed animals gradually became weak and suffered from hair loss with the progress of treatment. Unlike the control ones, livers from copper-exposed animals had a nailed appearance (indicated with arrows) on the external surface. Treatment with D-penicillamine (standard drug against copper toxicity) rectified this morphological alteration by an appreciable extent (Fig. 1C). This was supported by a significant decrease in ALT activity (Fig. 1D), and was eventually reflected in the increased survival of exposed animals after treatment with D-penicillamine (Fig. 1E).

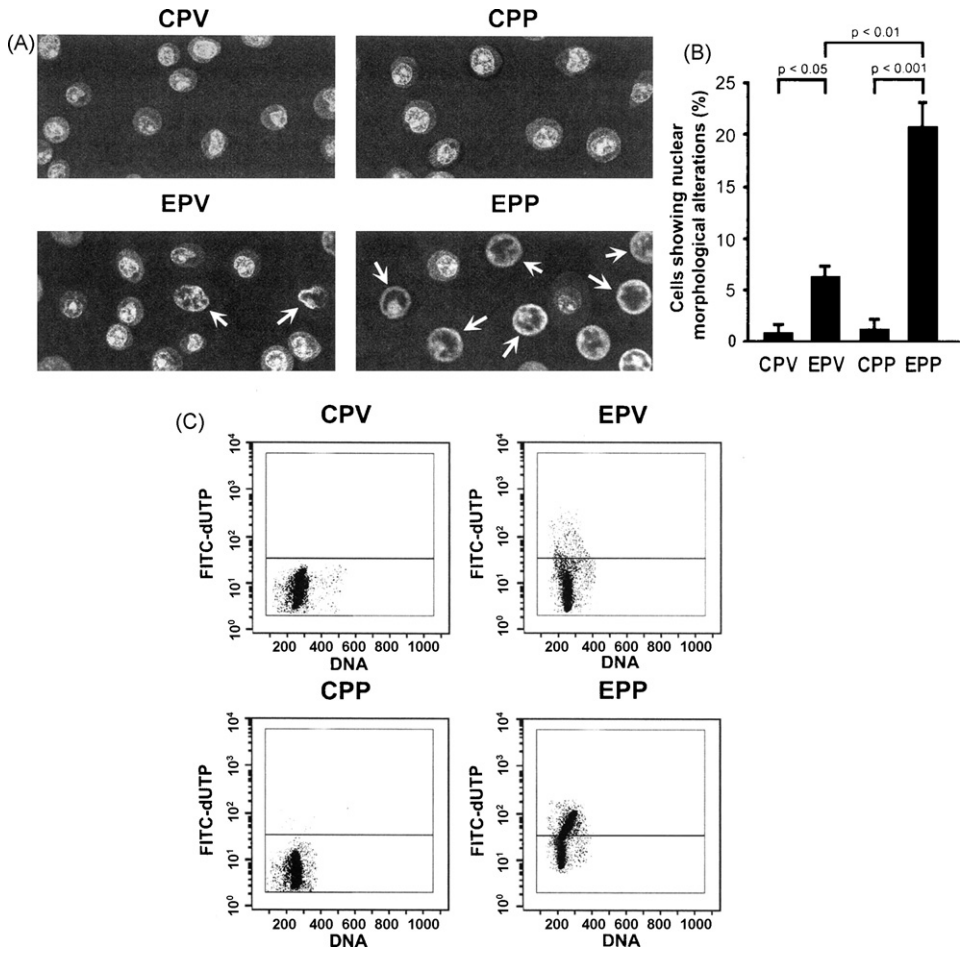

Fig. 4. Chronic exposure to copper leads to apoptotic changes in PP hepatocytes showing altered nuclear morphology and DNA fragmentation. (A) Nuclear morphology was assessed by staining the cells with membrane permeable fluorochrome H33342 and studied under the confocal microscope. Arrows indicate chromatin condensation and margination in copper-exposed (EPV and EPP) animals. The magnification of the photomicrograph is 400×. (B) Quantitative estimation of cells exhibiting altered nuclear morphology per 100 hepatocytes from PP and PV zones of control and copper-exposed animals. Results are the mean ± SD of three independent observations. (C) DNA fragmentation was determined by TUNEL assay as described in Section 2. FACS analysis demonstrates DNA end-labeling with FITC-dUTP, counter stained with PI. Cell aggregates were gated out with PI staining and FITC fluorescence was measured relative to a horizontal gate set by analysis of apoptotic and non-apoptotic hepatocytes. In control cells (CPV and CPP) FITC fluorescence was minimal (i.e. below the gate) whereas it was significantly more apparent in PP cells (EPP) compared to PV cells (EPV) in response to copper exposure. Results are representative of five independent experiments.

3.2. Zonal heterogeneity in copper accumulation affecting liver histology during chronic exposure

Interestingly, histological studies showed copper-induced cellular injury with greater damage in the periportal (PP) region in comparison to the perivenous (PV) region within the liver acinus. A detailed study of the PP region revealed fibrotic (F) changes (indicated with arrows) with the formation of prominent bile plugs (BP) (Fig. 2A). This was accompanied by parenchymal collapse which was replaced by cholangiolar proliferation (Fig. 2B). Images taken under higher magnification (Fig. 2C) show ballooning of hepatocytes (BL) and mallory body (ML) formation (indicated with arrows). Severity of hepatic injury in the PP region may be correlated with the preferential accumulation of copper in this region in comparison to the PV region (Fig. 3A). Staining with Rhodanine further confirmed the deposition of copper in the PP region (Fig. 3B).

3.3. Copper toxicity disrupts nuclear morphology of hepatocytes

Ultra structural studies with Hoechst 33342 revealed a marked alteration in the nuclear morphology. Fig. 4A shows a propensity towards chromatin condensation and margination (indicated with arrows) in the PP zone of the liver from the exposed group. Quantitation of this result (Fig. 4B) revealed a significant increase in the percentage of affected hepatocytes in the PP region (21.3%) in comparison to that in the PV region (6.5%). To assess the extent of copper-mediated apoptotic changes in the cells in terms of DNA strand breakage, we have measured FITC-dUTP DNA end-labeling by FACS analysis. Between the two zones, exposed cells from the PP region showed much higher labeling representing fragmented DNA. No significant labeling was observed in the cells from the control group (Fig. 4C).

3.4. Oxidative stress in hepatocytes in response to copper toxicity

DNA has been shown to get damaged through oxidative stress under various adverse situations [10]. Considering the involvement of copper in the induction of oxidative stress via the Fenton reaction [11], our next experiment was to find out whether this disparity in liver damage between the two zones resulted from a difference in the development of oxidative stress in these zones. True to our expectation, Fig. 5A indicates a significant increase in TBARS level in the exposed periportal (EPP) zone over the exposed perivenous (EPV) zone. To determine the involvement of ROS in copper-mediated redox imbalance in liver cells, we used fluorogenic probes DHE and DCFDA to detect superoxide and hydrogen

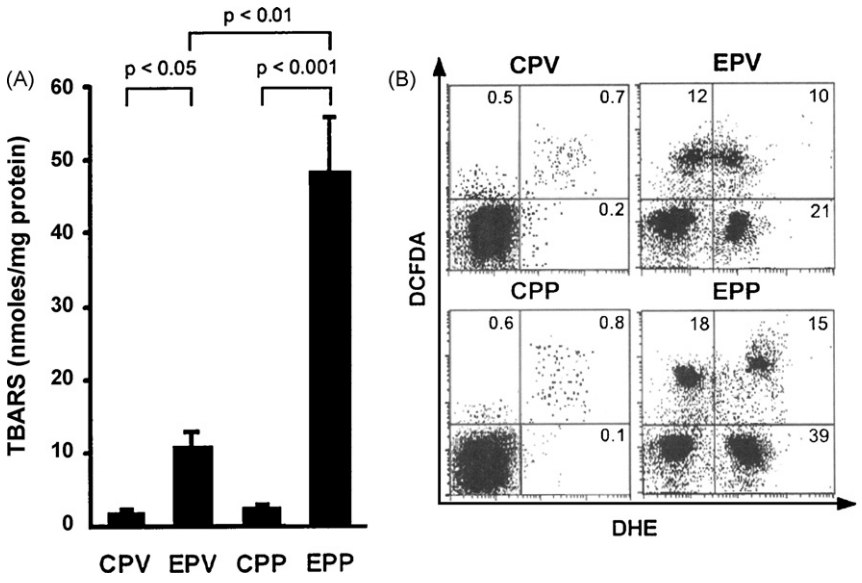

Fig. 5. Copper-mediated oxidation of membrane lipids and generation of ROS in hepatocytes. (A) Copper increases oxidative stress on membrane lipids of PP hepatocytes showing enhanced TBARS production. Results are the mean ± SD of three independent experiments. (B) Dot plots are the results of FACS analysis after binding of hepatocytes (1×10^5) to DCFDA and DHE for determining H_2O_2 and $O_2^{\bullet -}$ generation respectively, as described in Section 2. Copper treatment leads to a marked increase in $O_2^{\bullet -}$ generation as evident from the increased binding of DHE in the lower right quadrant of the right panel. Results are representative of three independent experiments.

peroxide respectively. About 2% of the cells from PP and PV regions of the control group exhibited fluorescence (left panel of Fig. 5B) indicating a basal level of ROS production. The panel further shows a comparable distribution of both DHE and DCFDA fluorescence, representing superoxide and hydrogen peroxide respectively, in these two regions. Copper exposure led to a large increase in the production of ROS although their distribution varied widely among the population of the cells belonging to PP and PV zones (Right panel of Fig. 5B). Cells located in the upper left quadrant exhibited only DCFDA, whilst those in the upper right quadrant exhibited both DCFDA and DHE fluorescence. There was a 5–6% increase in these two populations of cells obtained from the PP region over that from the PV region. However, maximum increase was observed in the superoxide producing cells located in the lower right quadrant, exhibiting only DHE fluorescence. The figure shows an increase of fluorescence by about 72% from the basal level in the EPP zone in comparison to an increase of about 43% in the EPV zone.

3.5. Hepatocytes from PP region exhibit downregulation of SOD and upregulation of GSH oxidation in copper toxicity

Considering the contribution of cytosolic antioxidants in maintaining the redox balance in the cells, we next measured the status of Cu-Zn SOD and GSH/GSSG ratio in the cytosolic compartment of the cells isolated from the PP and PV regions. As evident from Fig. 6A, decrease in the activity of Cu-Zn SOD after copper exposure was much more pronounced for EPP cells (90%) than EPV cells (30%) from the corresponding control levels. The decrease of Cu-Zn SOD activity may come from degradation of Cu-Zn SOD in EPP cells, a possibility supported by immunoblots in Fig. 6B, but other alternatives exist.

Glutathione (GSH) is an important member of the cellular antioxidant family and along with SOD it also functions as an efficient intracellular radical scavenger. Paradoxically, GSH can also act as a prooxidant by undergoing auto oxidation and producing ROS through a metal (specifically copper) catalyzed reaction [35]. Fig. 6C shows a significant decrease of the GSH/GSSG ratio indicating the oxidation of GSH to GSSG after copper exposure. The effect was more prominent in the EPP cells and suggests its likely contribution in copper-mediated enhanced production of superoxide in these cells. Since mitochondria plays a major role in ROS induced cell death [34], we next measured the activity of mitochondrial SOD or Mn SOD along with the redox status of glutathione in response to copper exposure in this organelle. The pattern of alteration in mitochondrial SOD was more or less similar to the cytosolic SOD although the extent of depletion in Mn SOD was a little less than that of Cu-Zn SOD (Fig. 6D). Copper-catalyzed oxidation of GSH was negligible in mitochondria from the PV region but quite significant in mitochondria from the PP region (Fig. 6E). The result indicates an active contribution of the antioxidant system in implicating mitochondria as a target for oxidant injury in copper-mediated hepatotoxicity.

3.6. Copper-mediated $O_2^{\bullet -}$ generation, dissipation of MMP, ATP depletion and permeabilization of mitochondrial membrane preferentially in the hepatotoxicity from the PP region

Involvement of copper in the enhanced oxidation of GSH in the PP zone was further supported by the increased mitochondrial copper accumulation in this zone (Fig. 7A). To determine whether the interaction of intracellular copper with GSH promotes the generation of superoxide, a possible candidate for inflicting oxidative stress during copper exposure, we measured the superoxide level in the mitochondria using the specific fluorogenic probe DHE. Fig. 7B, showing a sharp increase in the superoxide level in the EPP cells, indicated the involvement of this ROS in the process. Since the electrochemical potential of the proton gradient, generated across the mitochondrial membrane ($\Delta\psi_m$), has been shown to be sensitive to the redox state of the cells [34], our next experiment was to determine the effect of copper exposure on $\Delta\psi_m$ in hepatocytes isolated from different zones of the liver. This was done by monitoring the fluorescence quenching of Rhodamine 123 (Rh-123) by FACS analysis. Cells isolated from exposed animals (EPP and EPV) depicted weaker fluorescence compared to the bright fluorescence in cells from the control group (CPP and CPV), indicating a reduction in $\Delta\psi_m$ following copper treatment (Fig. 7C). Quenching of Rh-123 was much higher in EPP cells, pointing to a greater mitochondrial depolarization in these cells. Fig. 7D shows the effect of copper treatment on ATP generation consequent to mitochondrial dysfunction. As expected, the extent of ATP deple-

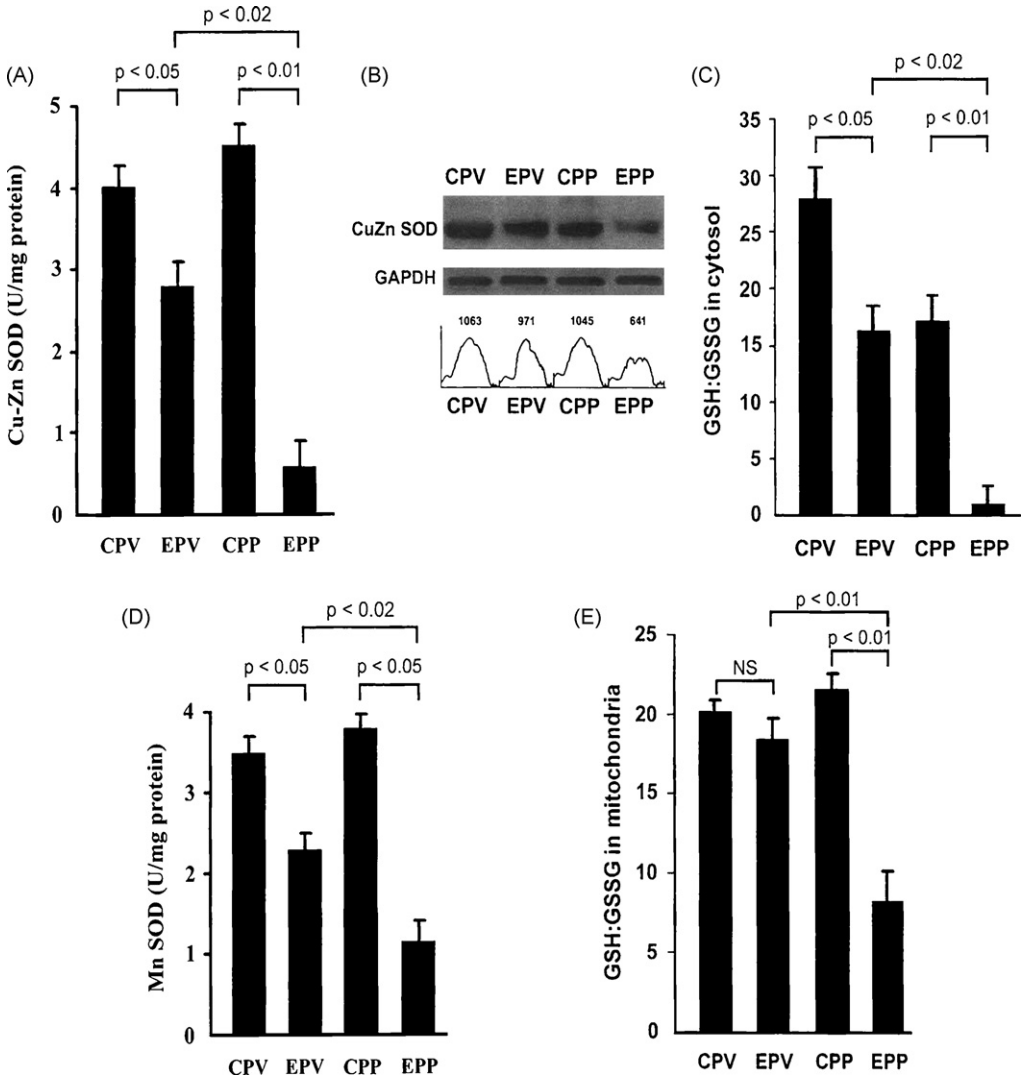

Fig. 6. Copper exposure impairs the functioning of SOD and glutathione systems in hepatocytes. (A) Downregulation of cytosolic Cu-Zn SOD and (D) mitochondrial Mn SOD in the hepatocytes of copper-exposed animals from their respective control levels. The effect was significantly more pronounced in the PP region (EPP cells). SOD was assayed by measuring 50% inhibition of $O_2^{\bullet -}$-mediated oxidation of pyrogallol as described in Section 2. Results are the mean ± SD of three independent experiments. (B) Representative Western blot of Cu-Zn SOD isolated from the cytosolic fractions of hepatocytes. (C) Glutathione levels in cytosolic fraction and (E) in mitochondrial fraction of hepatocytes were estimated as described in Section 2. Copper-mediated decrease of GSH/GSSG ratio being more prominent in cytosol points towards a prooxidant role of cytosolic GSH in the generation of $O_2^{\bullet -}$ in the PP hepatocytes. Results are the mean ± SD of three independent experiments.

tion followed a similar trend as the loss of $\Delta\psi_m$ in cells collected from the two zones of liver. The figure shows a partial decrease (about 50%) of ATP generation from the control level in EPP cells, that suggests apoptotic changes in these cells after copper exposure. MPT pore opening, following mitochondrial depolarization and ATP depletion, has been reported to be a sensitive mechanism of mitochondrial injury which eventually proceeds to apoptotic death of the cells [36]. Copper exposure led to a marked increase in the permeabilization of mitochondrial membrane from the control level, as assessed from the amplitude of mitochondrial swelling over 15 min (Fig. 7E). Consistent with the higher rate of superoxide production, the swelling was much faster in EPP cells (light blue scan) compared to EPV cells (red scan).

3.7. Copper promotes glutathione-dependent $O_2^{\bullet -}$ generation and dissipation of $\Delta\psi_m$ in hepatocytes

Involvement of cytosolic GSH in copper-induced superoxide generation and dissipation of $\Delta\psi_m$ was further examined under *in vitro* conditions. To this end, we first ensured the bioavailability of copper within the cytosol after incubation of PP cells with different concentrations of copper (Fig. 8A). This figure shows a concentration-dependent rise in intracellular copper accumulation which reached a steady level of about 8.5 nmol/mg protein in response to incubation with 100 μM $CuSO_4$. From this result we used a copper concentration of 80 μM for our further incubations, which led to accumulation of about 8 nmol of copper/mg protein, a level compatible with that obtained in the cytosol in response to *in vivo* copper treatment (Fig. 3A). Fig. 8B shows a steady rise in copper-induced superoxide generation over time in the cytosol (red scan) which was further stimulated in presence of the SOD inhibitor DETC (light blue scan). The absolute need of GSH as a reducing agent in this system was established by oxidizing GSH with glutathione peroxidase (GPx) and hydrogen peroxide (H_2O_2), which limited the source of GSH in the incubation mixture. With this limited supply of GSH, copper failed to increase the fluorescence (dark blue scan) over the base line level of superoxide production in the cytosol (green scan). The inset shows the levels of GSH and GSSG before and after oxidation of GSH in the incubation system (corresponding to green and dark blue scans respectively). The effect of GSH oxidation

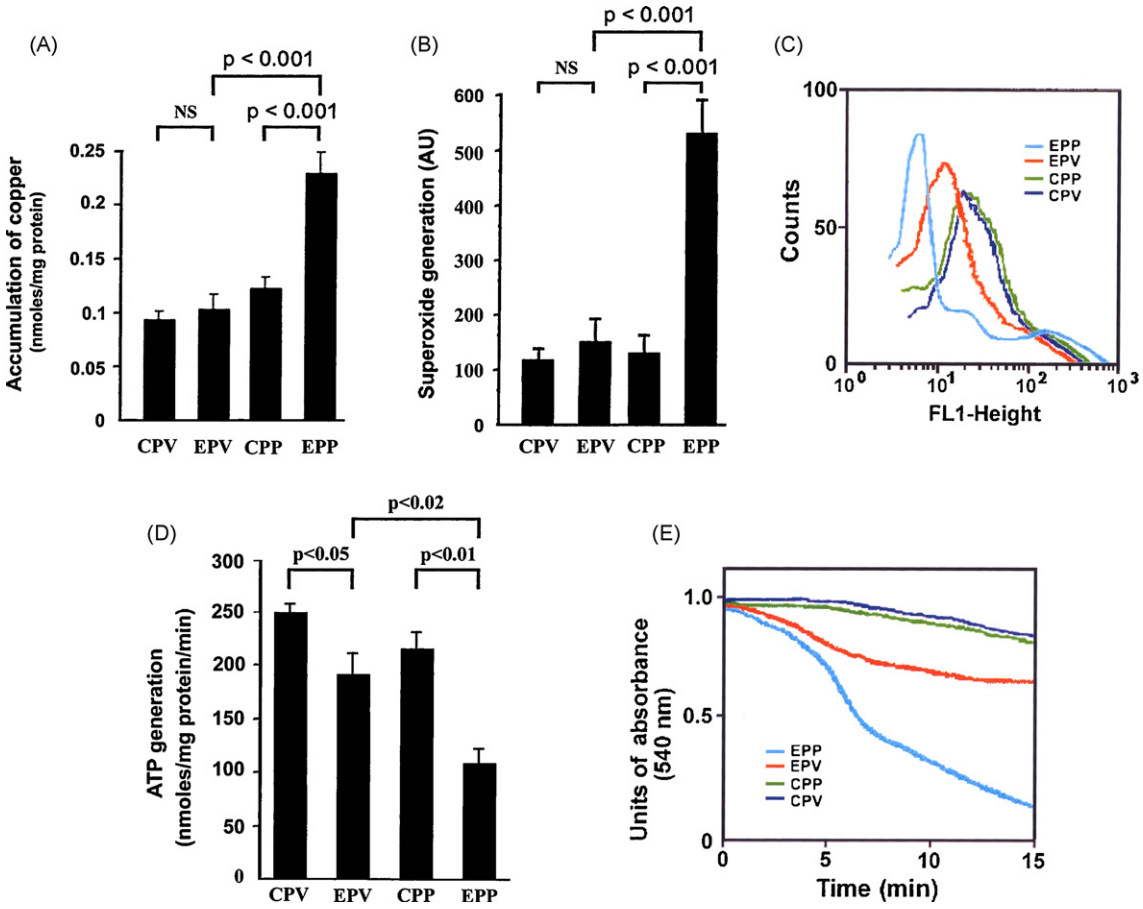

Fig. 7. Copper exposure leads to ROS generation, energy depletion and mitochondrial dysfunction in hepatocytes. (A) Accumulation of copper in the mitochondrial fraction of hepatocytes collected from PP and PV regions were estimated in AAS. (B) Mitochondrial $O_2^{\bullet -}$ generation was assessed using the fluorescent probe DHE as described in Section 2. Fluorescence was quantified as a measure of $O_2^{\bullet -}$ generation and expressed in arbitrary unit (AU). (C) Dissipation of MMP was estimated from the quenching of Rhodamine 123 from FACS analysis as described in Section 2. Copper exposure increases the quenching in EPP (light blue scan) and EPV (red scan) cells indicating greater depolarization of membrane potential in comparison to that in their unexposed counterparts i.e. CPP (green scan) and CPV (dark blue scan) cells respectively. (D) ATP production in mitochondria was determined by luminescence (luciferin/luciferase) assay as described in Section 2. ATP production levels were quantified as nmol of ATP/mg of mitochondrial protein/min. (E) MPT in the hepatocytes was assessed from the changes in amplitude of mitochondrial swelling over time as described in Section 2. Copper exposure increases the rate of mitochondrial swelling in EPP (light blue scan) and EPV (red scan) cells compared to that in their unexposed counterparts, CPP (green scan) and CPV (dark blue scan), as evident from the decrease of absorbance at 540 nm with time. Results presented in each of the panels (A), (B), and (D) are the mean ± SD of five independent experiments and the results in panels (C) and (E) are representative of three independent experiments each. (For interpretation of the references to color in this figure legend, the reader is referred to the web version of the article.)

on copper-induced superoxide formation was further reflected in the dissipation of $\Delta\psi_m$ (Fig. 8C). The dissipation was effectively inhibited by oxidizing GSH (dark blue scan) and restricted to the base line level (green scan), in contrast to the sharp reduction of fluorescence indicating mitochondrial depolarization in presence of GSH and copper (red scan).

4. Discussion

Copper is an essential transition metal which is required for normal growth and development of living organisms. It functions as a cofactor for several mammalian enzymes like cytochrome C oxidase, Cu-Zn SOD, and ceruloplasmin [37]. Hepatocellular copper homeostasis involves copper uptake into hepatocytes followed by its incorporation into major copper containing proteins and excretion through bile [4]. When copper accumulation surpasses the normal storage capacity of the liver, it causes hepatocellular injury and cell death [5]. Previous reports emphasize copper-induced cell death that involves ROS mediated mitochondrial dysfunction [38]. Copper overload brings about a regional variation in its distribution whose effect gets reflected in the development of a zonal difference towards liver injury. This is in accordance with the previous reports on the accumulation of copper exclusively in the PP region of rat liver that brings about cellular degeneration in this region in copper storage disease [39–41]. However, till date, very few efforts have been made to explore the factors responsible for this differential damage between cells from PP and PV zones during copper toxicity under *in vivo* conditions. Vulnerability of the PP region to copper toxicity may be explained to some extent from the potential role of kupffer cells which show a functional heterogeneity in relation to their position in the liver acinus. Kupffer cells, the resident macrophages in liver, play significant roles in immuno modulation, phagocytosis and biochemical attack [42]. Copper supplementation alters the functional status of kupffer cells by enhancing their respiratory burst activity along with the release of biologically active products related to cell injury [43,44]. Kupffer cells from the PP region are reported to exhibit high endocytic activity and greater lysosomal enzyme activities as compared to PV kupffer cells. Moreover, increased (3–4 times more) distribution of these cells in the PP region over PV region [45] is likely to contribute to the development of hepatocellular injury preferentially in the PP region during copper toxicity. This is the first report unfolding the underlying mechanism behind the distinctive pattern of damage in different zones, starting from copper accumulation and ending in the death of hepatocytes.

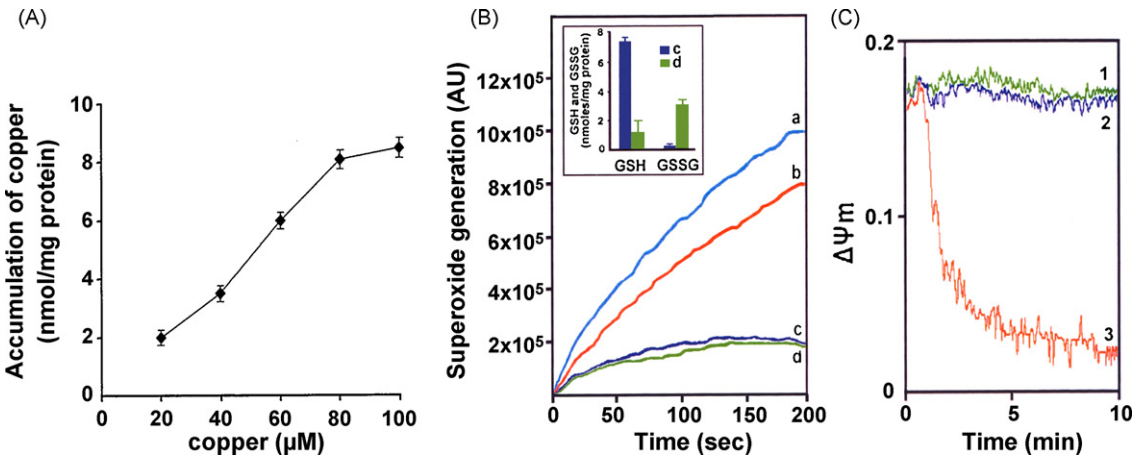

Fig. 8. Oxidation of cytosolic GSH inhibits copper-induced $O_2^{\bullet-}$ generation and dissipation of $\Delta\psi_m$. Hepatocytes isolated from PP region were maintained on 12-well tissue culture plates containing complete RPMI 1640 medium at 37 °C in 5% CO_2. (A) Primary cultured hepatocytes were treated with $CuSO_4$ of increasing concentrations ranging from 20 to 100 μM. After 24 h cells were collected from the culture media and washed with PBS (pH 7.4). Amounts of copper in the medium after the incubation period were measured by AAS. (B) Cytosol of hepatocytes was used as the source of GSH in this experiment. Superoxide generation was monitored for 200 s after addition of DHE (10 μM in DMSO) in final incubation medium, in presence of air at 37 °C under shaking condition. (a) Cytosol was incubated with SOD inhibitor (100 μM DETC) for 5 min, and copper was then added at a concentration of 8 nmol/mg protein (light blue scan). (b) Copper (8 nmol/mg protein) was added to the cytosol (red scan). (c) Cytosol was incubated with H_2O_2 (0.2 mM) and GPx (2 mM) for 10 min then copper (8 nmol/mg protein) was added (dark blue scan). (d) Only cytosol (green scan). In the inset figure, the ratio of GSH and GSSG was quantified under the conditions given in (c) and (d). (C) Rhodamine 123 (1 μM) was used to estimate changes in MMP ($\Delta\psi_m$) for a period of 10 min in a spectrofluorimeter. In this experiment lysate was used as mitochondrial source. Cultured hepatocytes were lysed by sonication in HEPES buffer, pH 7.5 containing 0.25 M sucrose, 5 mM EDTA, 10 mM mercaptoethanol, 2 mM PMSF and 1 mM leupeptin.1, only lysate (green scan) 2, lysate was incubated with H_2O_2 (0.2 mM) and GPx (2 mM) for 10 min under shaking condition at 37 °C and then copper (8 nmol/mg protein) was added into the sample 30 min before measuring $\Delta\psi_m$ (dark blue scan). 3, lysate was incubated with copper (8 nmol/mg protein) for 30 min before measuring $\Delta\psi_m$ (red scan). Results are representative of six independent experiments. (For interpretation of the references to color in this figure legend, the reader is referred to the web version of the article.)

Chronic administration of copper at the dose of 15 mg/kg for 45 days produced significant liver injury and provided us with a suitable model for studying the mechanism of copper-induced hepatotoxicity under *in vivo* conditions. In accordance with previous reports [39,46], histological and histochemical analyses revealed a distinctive pattern of liver damage in consequence of uneven distribution of copper at the acinar level. Since biliary excretion plays a major role in the homeostatic regulation of copper [47,40], an excessive burden of the metal in the liver is likely to disturb the normal excretion process which eventually leads to bile stasis and PP copper retention causing cellular injury. Furthermore, hepatocellular damage at the PP region gives an indication of chronic copper toxicosis under the experimental conditions.

Copper toxicity has been reported to result from redox imbalance and is connected to the generation of ROS. Within the cell, cupric ions target thiol groups resulting in the reduction of Cu^{2+} to Cu^{1+} and oxidation of thiols to disulphides. Cu^{1+} ions formed are then reoxidized to Cu^{2+} in presence of molecular oxygen. Molecular oxygen is thereby converted to $O_2^{\bullet-}$ with subsequent formation of H_2O_2 and $^{\bullet}OH$ radicals via the Fenton reaction [11,48]. GSH is present at high concentrations in the cells and body fluids. It scavenges various ROS, reduces substrates for peroxidases and thus helps to maintain a reduced state within the aerobic cells against oxidant threat. Paradoxically, thiols also behave as prooxidants by donating electrons in a nonenzymatic metal-catalyzed oxidation system, resulting in the generation of ROS [35]. This explains increased production of ROS in association with decreased GSH/GSSG ratio in the PP region following copper overload and implicates copper-mediated thiol oxidation in the system.

Although copper has been reported to induce significant increase in the generation of both $O_2^{\bullet-}$ and H_2O_2 in an *in vitro* system [49], here we have found a predominant role of $O_2^{\bullet-}$ in inflicting copper-mediated hepatotoxicity under *in vivo* conditions. This may be reasoned out as an anticipated consequence of decreased functioning of cytosolic Cu-Zn SOD as observed in the present study. Cu-Zn SOD is a metalloenzyme, essential for the dismutation of $O_2^{\bullet-}$ to H_2O_2 [50]. Although the decrease in EPP cells of both Cu-Zn SOD activity (Fig. 6A) and protein content (Fig. 6B) may arise from an increase in protein degradation, owing to copper-mediated over-production of superoxide [51,52], the notable nuclear damage caused by copper toxicity in PP cells (Fig. 4) makes it possible that the drop of Cu-Zn SOD activity and protein reflects changes in gene expression, at transcriptional or translational levels [53,54], a possibility that deserves further studies.

Since mitochondria plays a key role in controlling both cell survival and cell death [9], our next attempt was to determine mitochondrial alteration developed in the cells from PP and PV regions following the generation of ROS in the system. Liver injury was accompanied by reduction in Mn SOD activity and altered mitochondrial thiol–disulphide ratio, suggesting oxidative stress in mitochondria to be a likely cause for hepatotoxicity produced

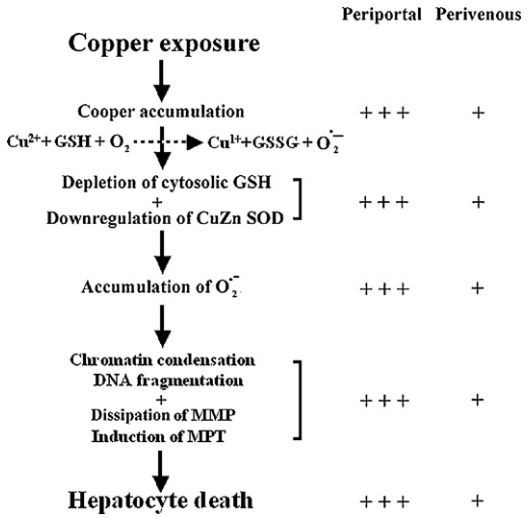

Fig. 9. Schematic representation of biochemical basis for the regional differences in copper-mediated hepatotoxicity.

by copper in an *in vivo* model. This was substantiated in a subsequent experiment, showing increased accumulation of copper in association with enhanced generation of $O_2^{\bullet-}$ in the mitochondria resulting from copper treatment.

Mitochondrial dysfunction was evident from collapse of $\Delta\psi_m$ as an outcome of permeabilization of the inner mitochondrial membrane [9]. Fall in ATP content was indicative of energy depletion, an expected consequence of mitochondrial dysfunction resulting from dissipated mitochondrial membrane potential [32]. Apoptosis, being an energy requiring process, requires a minimum level of ATP generation in contrast to necrosis, associated with complete depletion of ATP [55]. So our data showing partial depletion of ATP (50%) suggests copper-mediated apoptotic death of liver cells. Opening of MPT pore is an important event in the apoptotic death of liver cells [36]. However, greater generation of ROS, lower $\Delta\psi_m$ and increased depletion of ATP in the PP region provide a more favourable environment in this zone compared to the PV zone for MPT induction that eventually leads to mitochondrial swelling, disruption of the outer membrane and release of apoptotic factors [34].

Metal-catalyzed thiol depletion has been reported to cause imbalance in the prooxidant and antioxidant systems leading to oxidative stress, which in turn affects a number of cellular functions promoting apoptotic death of the cells [56]. This is in accordance with our observation showing depletion of GSH and generation of $O_2^{\bullet-}$ due to copper overloading under *in vivo* conditions. The effect, being more pronounced in the PP region, appears to be a possible reason for copper-mediated enhanced liver cell apoptosis in this region over the PV region. This observation was further strengthened in an *in vitro* experiment, where oxidation of GSH in presence of GPx and H_2O_2 was effective in restricting copper-induced $O_2^{\bullet-}$ generation and dissipation of $\Delta\psi_m$ to the basal level, thereby emphasizing the importance of cytosolic GSH in the reaction.

In conclusion, this study elucidated the biochemical basis for zonal differences in copper-mediated morphological and histological alterations in the liver cells that eventually leads to their apoptotic death during chronic exposure under *in vivo* conditions (Fig. 9). Working in this direction, we have identified $O_2^{\bullet-}$ to be primarily responsible for causing the damage. Our results further indicate the contribution of decreased SOD activity and perturbation in GSH/GSSG homeostasis in this process.

Conflict of interest statement

The authors declare that there are no conflicts of interest.

Acknowledgments

Authors are grateful to Dr. Anil Ghosh of Drug Development Diagnostics & Biotechnology Division and Dr. S.N. Kabir of Cell Biology & Physiology Division at the Indian Institute of Chemical Biology, Kolkata, for providing facilities for histological & microphotographic studies. Authors thank Mrs. Banasri Das for confocal microscopic studies. This work was supported by Council of Scientific and Industrial Research (CSIR), India, Project NWP 0009, and CSIR fellowships (to D.N.R. and S.M.).

References

[1] H. Popper, S. Goldfisher, I. Sternlieb, N.C. Nayak, T.V. Madhavan, Cytoplasmic copper and its toxic effects. Studies in Indian childhood cirrhosis, Lancet 1 (1979) 1205–1208.
[2] I. Sternlieb, Copper and the liver, Gastroenterology 78 (1980) 1615–1628.
[3] I.H. Scheinberg, I. Sternlieb, Wilson's Disease, WB Saunders, Philadelphia, 1984.
[4] J.R. Turnlund, Human whole-body copper metabolism, Am. J. Clin. Nutr. 67 (1998) 960S–964S.
[5] I.H. Scheinberg, I. Sternlieb, Wilson disease and idiopathic copper toxicosis, Am. J. Clin. Nutr. 63 (1996) 842S–845S.
[6] P.G. Traber, J. Chianale, J.J. Gumucio, Physiologic significance and regulation of hepatocellular heterogeneity, Gastroenterology 95 (1988) 1130–1143.
[7] K. Jungermann, N. Katz, Functional specialization of different hepatocyte populations, Phys. Rev. 69 (1989) 708–764.
[8] C.T. Sheline, D.W. Choi, Cu^{2+} toxicity inhibition of mitochondrial dehydrogenases *in vitro* and *in vivo*, Ann. Neurol. 55 (2004) 645–653.
[9] G. Kroemer, J.C. Reed, Mitochondrial control of cell death, Nat. Med. 6 (2000) 513–519.
[10] B. Halliwell, J.M.C. Gutteridge, Role of free radicals and catalytic metal ions in human disease: an overview, Method Enzymol. 186 (1990) 1–85.
[11] E.D. Harris, Basic and clinical aspects of copper, Crit. Rev. Clin. Lab. Sci. 40 (2003) 547–586.
[12] P.J. Aggett, An overview of the metabolism of copper, Eur. J. Med. Res. 4 (1999) 214–216.
[13] J. Evans, H. Zerpa, L. Nuttall, M. Boss, S. Sherlock, Copper chelation therapy in intrahepatic cholestasis of childhood, Gut 24 (1983) 42–48.
[14] M.D. Lorenz, L.M. Cornelius, D. Ferguson, Small Animal Medical Therapeutics, Wiley-Blackwell Publishers, 1992.
[15] G.J. Brewer, The risks of free copper in the body and the development of useful anticopper drugs, Curr. Opin. Clin. Nutr. Metab. Care 11 (2008) 727–732.
[16] P.O. Seglen, Preparation of isolated rat liver cells, Methods Cell Biol. 13 (1976) 29–83.
[17] K.O. Lindros, K.E. Penttila, Digitonin-collagenase perfusion for efficient separation of periportal or perivenous hepatocytes, Biochem. J. 228 (1985) 757–760.
[18] H. Sasaki, H. Kume, A. Nemoto, S. Narisawa, N. Takahashi, Ethanolamine modulates the rate of rat hepatocyte proliferation in vitro and in vivo, Proc. Natl. Acad. Sci. U.S.A. 94 (1997) 7320–7325.
[19] V.K.S. Tay, A.S. Wang, K.Y. Leow, M.M.K. Ong, K.P. Wong, U.A. Boelsterli, Mitochondrial permeability transition as a source of superoxide anion induced by the nitroaromatic drug nimesulide in vitro, Free Radic. Biol. Med. 39 (2005) 949–959.
[20] C. Domenicotti, D. Paola, A. Vitali, M. Nitti, D. Cottalasso, E. Melloni, G. Poli, U.M. Marinari, M.A. Pronzato, Mechanisms of inactivation of hepatocyte protein kinase C isoforms following acute ethanol treatment, Free Radic. Biol. Med. 25 (1998) 529–535.
[21] M. Harashima, K. Harada, Y. Ito, M. Hyuga, T. Seki, T. Ariga, T. Yamaguchi, S. Niimi, AnnexinA3 expression increases in hepatocytes and is regulated by hepatocyte growth factor in rat liver regeneration, J. Biochem. 143 (2008) 537–545.
[22] J. Nair, S. Strand, N. Frank, J. Knauft, H. Wesch, P.R. Galle, H. Bartsch, Apoptosis and age-dependant induction of nuclear and mitochondrial etheno-DNA adducts in Long-Evans Cinnamon (LEC) rats: enhanced DNA damage by dietary curcumin upon copper accumulation, Carcinogenesis 26 (2005) 1307–1315.
[23] A.L. Hubbard, D.A. Wall, A. Ma, Isolation of rat hepatocyte plasma membranes. 1. Presence of the three major domains, J. Cell Biol. 96 (1983) 217–229.
[24] M.H. Wisher, W.H. Evans, Functional polarity of the rat hepatocyte surface membrane, isolation and characterization of plasma-membrane subfractions from the blood-sinusoidal, bile-canalicular and contiguous surfaces of the hepatocyte, Biochem. J. 146 (1975) 375–388.
[25] U. Rauen, B. Polzar, S. Stephan, H.G. Mannherz, H.D. Groot, Cold-induced apoptosis in cultured hepatocytes and liver endothelial cells: mediation by reactive oxygen species, FASEB J. 13 (1999) 155–168.
[26] J.P. Silva, I.G. Shabalina, E. Dufour, N. Petrovic, E.C. Backlund, K. Hultenby, R. Wibom, J. Nedergaard, B. Cannon, N. Larsson, SOD2 overexpression: enhanced mitochondrial tolerance but absence of effect on UCP activity, EMBO J. 24 (2005) 4061–4070.
[27] G. Sen, D. Biswas, M. Ray, T. Biswas, Albumin-quercetin combination offers a therapeutic advantage in the prevention of reduced survival of erythrocytes in visceral leishmaniasis, Blood Cells Mol. Dis. 39 (2007) 245–254.
[28] F. Tietze, Enzymatic method for quantitative determination of nanogram amounts of total and oxidized glutathione: applications to mammalian blood and other tissues, Anal. Biochem. 27 (1969) 502–522.
[29] S.K. Srivastava, E. Beutler, Accurate measurement of oxidized glutathione content of human, rabbit, and rat red blood cells and tissues, Anal. Biochem. 25 (1968) 70–76.
[30] S. Marklund, G. Marklund, Involvement of the superoxide anion radical in the autoxidation of pyrogallol and a convenient assay for superoxide dismutase, Eur. J. Biochem. 47 (1974) 469–474.
[31] J.L. Mauriz, M. Virginia, V.G. Maria, G. Paquita, P.B. Juan, G.G. Javier, Melatonin prevents oxidative stress and changes in antioxidant enzyme expression and activity in the liver of aging rats, J. Pineal Res. 42 (2007) 222–230.
[32] B.D. Follstad, D.I.C. Wang, G. Stephanopoulos, Mitochondrial membrane potential differentiates cells resistant to apoptosis in hybridoma cultures, Eur. J. Biochem. 267 (2000) 6534–6540.
[33] R.K. Emaus, R. Grunwald, J.J. Lemasters, Rhodamine123 as a probe of transmembrane potential in isolated rat liver mitochondria: spectral and metabolic properties, Biochem. Biophys. Acta 850 (1986) 436–448.
[34] A. Bernareggi, Clinical pharmacokinetics of nimesulide, Clin. Pharmacokin. 35 (1998) 247–274.
[35] A.V. Kachur, C.J. Koch, J.E. Biaglow, Mechanism of copper-catalyzed oxidation of glutathione, Free Radic. Res. 28 (1998) 259–269.
[36] H. Higuchi, M. Adachi, S. Miura, G.J. Gores, H. Ishii, The mitochondrial permeability transition contributes to acute ethanol-induced apoptosis in rat hepatocytes, Hepatology 34 (2001) 320–328.

[37] M. Arredondo, M.T. Núñez, Iron and copper metabolism, Mol. Aspects Med. 26 (2005) 313–327.
[38] N.L. Saris, I.A. Skulskii, Interaction of Cu^{+} with mitochondria, Acta Chem. Scand. 45 (1991) 1042–1046.
[39] I. Fuentealba, S. Haywood, J. Trafford, Variations in the intralobular distribution of copper in the livers of copper-loaded rats in relation to the pathogenesis of copper storage diseases, J. Comp. Pathol. 100 (1989) 1–11.
[40] S. Haywood, T. Müller, W. Müller, P. Heinz-Erian, M.S. Tanner, G. Ross, Copper-associated liver disease in North Ronaldsay sheep: a possible animal model for non-Wilsonian hepatic copper toxicosis of infancy and childhood, J. Pathol. 195 (2001) 264–269.
[41] I. Bykov, P. Ylipaasto, L. Eerola, K.O. Lindros, Functional differences between periportal and perivenous kupffer cells isolated by digitonin-collagenase perfusion, Comp. Hepatol. 3 (Suppl. 1) (2004) S34.
[42] L.A. Videla, V. Fernández, G. Tapia, P. Varela, Oxidative stress-mediated hepatotoxicity of iron and copper: role of kupffer cells, BioMetals 16 (2003) 103–111.
[43] S. Jorge, A. Maria, F. Paola, T. Pilar, F. Virginia, A.L. Videla, Influence of copper-(II) on colloidal carbon-induced kupffer cell-dependent oxygen uptake in rat liver: Relation to hepatotoxicity, Free Radic. Res. 30 (1999) 489–498.
[44] F.A. Cisternas, T. Gladys, A. Miguel, C.U. Denise, P. Romanque, W.D. Sierralta, M.T. Vial, L.A. Videla, M. Araya, Early histological and functional effects of chronic copper exposure in rat liver, BioMetals 18 (2005) 541–551.
[45] E.C. Sleyster, D.L. Knook, Relation between localization and function of rat liver kupffer cells, Lab. Invest. 47 (1982) 484–490.
[46] J.C. Wilton, J.K. Chipman, C.J. Lawson, A.J. Strain, R. Coleman, Periportal and perivenous enriched hepatocyte couplets: differences in canalicular activity and in response to oxidative stress, Biochem. J. 292 (1993) 773–779.
[47] I.C. Fuentealba, J.E. Mullins, E.M. Aburto, J.C. Lau, G.M. Cherian, Effect of age and sex on liver damage due to excess dietary copper in Fischer 344 rats, Clin. Toxicol. 38 (2000) 709–717.
[48] L.M. Gaetke, C.K. Chow, Copper toxicity, oxidative stress, and antioxidant nutrients, Toxicology 189 (2003) 147–163.
[49] Y. Ohta, N. Shiraishi, T. Nishikawa, M. Nishikimi, Copper-catalyzed auto oxidations of GSH and L-ascorbic acid: mutual inhibition of the respective oxidations by their coexistence, Biochim. Biophys. Acta Gen. Subjects 1474 (2000) 378–382.
[50] C. Lin, J. Kang, R. Zheng, Oxidative stress is involved in inhibition of copper on histone acetylation in cells, Chem. Biol. Interact. 151 (2005) 167–176.
[51] C. Steinkühler, M.T. Carrì, G. Micheli, L. Knoepfel, U. Weser, G. Rotilio, Copper-dependent metabolism of Cu-Zn superoxide dismutase in human K562 cells. Lack of specific transcriptional activation and accumulation of a partially inactivated enzyme, Biochem. J. 302 (1994) 687–694.
[52] O.J. Kwon, S.M. Lee, R.A. Floyd, J.W. Park, Thiol-dependent metal-catalyzed oxidation of copper, zinc superoxide dismutase, Biochim. Biophys. Acta Protein Struct. Mol. Enzymol. 1387 (1998) 249–256.
[53] D.Y. Yu, W.F. Li, B. Deng, X.F. Mao, Effects of lead on hepatic antioxidant status and transcription of superoxide dismutase gene in pigs, Biol. Trace Elem. Res. 126 (2008) 121–128.
[54] J.L. Mauriz, V. Molpeceres, M.V. García-Mediavilla, P. González, J.P. Barrio, J.G. González, Melatonin prevents oxidative stress and changes in antioxidant enzyme expression and activity in the liver of aging rats, J. Pineal Res. 42 (2007) 222–230.
[55] J. Villena, M. Henriquez, V. Torres, F. Moraga, J. Díaz-Elizondo, C. Arredondo, M. Chiong, C. Olea-Azar, A. Stutzin, S. Lavandero, A.F.G. Quest, Ceramide-induced formation of ROS and ATP depletion trigger necrosis in lymphoid cells, Free Radic. Biol. Med. 44 (2008) 1146–1160.
[56] C.R. Faverney, A. Devaux, M. Lafaurie, J.P. Girard, B. Bailly, R. Rahmani, Cadmium induces apoptosis and genotoxicity in rainbow trout hepatocytes through generation of reactive oxygen species, Aquat. Toxicol. 53 (2001) 65–76.